

# Self-Oscillating Class-D Audio Amplifier With A Phase-Shifting Filter in Feedback Loop

Hyunsun Mo<sup>1</sup> and Daejeong Kim<sup>a</sup>

Department of Electronics Engineering, Kookmin University

E-mail : <sup>1</sup>tyche@kookmin.ac.kr

**Abstract** – A self-oscillating class-D audio amplifier adopting the phase-shifting loop filter in the feedback filter is proposed. To validate the design, a mathematical model is proposed. It is alleged in a very simple form which describes the switching frequency variation as the function of the modulation depth to be applied to any general structure: phase shifting, time delay of the loop, and the hysteresis window at the comparator. The main focus is set on the analysis of the phase-shifting filter which shows the least dependency on the modulation depth.

## I. INTRODUCTION

The demand for near 1-W audio amplifier vitalizes the study on self-oscillating class-D amplifiers (SODA)[1],[6],[7]. Fig. 1(a) shows a typical structure of SODA. The oscillation frequency is determined by the total time delay of the loop ( $t_D$ ), the hysteresis-based delay at the comparator ( $h$ ), and the bandwidth of the feedback filter ( $f_o$ ).

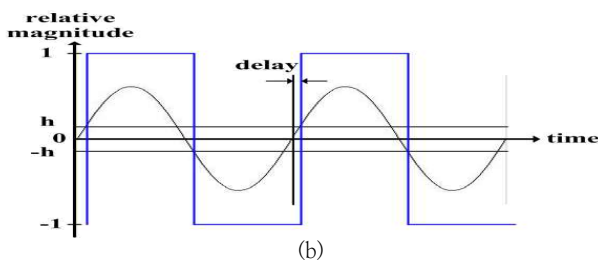
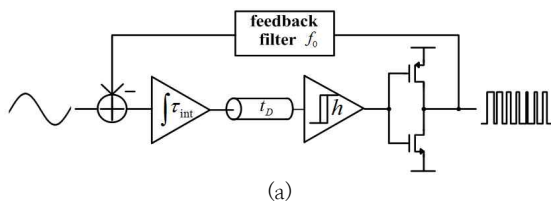


Fig. 1. Typical features of self-oscillating class-D amplifier (SODA) (a) basic structure (b) delay time generated in hysteresis window.

a. Corresponding author : Daejeong Kim; [kimdj@kookmin.ac.kr](mailto:kimdj@kookmin.ac.kr)

Copyright ©2015 IDEC All rights reserved. This is an Open-Access article distributed under the terms of the Creative Commons Attribution Non-Commercial License (<http://creativecommons.org/licenses/by-nc/3.0>) which permits unrestricted non-commercial use, distribution, and reproduction in any medium, provided the original work is properly cited.

A time delay can be effectively realized at the comparator as shown in Fig. 1(b), and possibly interpreted simply as  $h\tau_{int}$  ( $h$  is the hysteresis window,  $\tau_{int}$  is the time constant of the integrator) if the signal is linearly approximated.

The main feature of the self-oscillation scheme lies in a relatively lower switching (oscillating) frequency of several hundreds of kilo Hertz, tracking the input amplitude more or less. Thus, it generates less quantization noise and idle tones than a PWM or a delta-sigma modulator of the same order [1].

Mobile devices generally employ a filter-less method in which the pulse-width modulated output signal is not reconstructed [2, 3], thereby, the electromagnetic interference (EMI) should be taken into consideration. In this regard, it gets some advantage as the self-oscillated frequency is discovered spread, distributing its energy over a range of switching frequencies.

On the other side, the switching frequency variation is of a great concern for mobile applications. The differences in switching frequency may cause audible intermodulation in multi-channel systems. Sometimes, the switching frequency may be degraded down into the signal band as the modulation depth increases. Therefore, it is important to analyze the effect of the modulation depth on the switching frequency variation.

Previous works disclose models for the delay time or hysteresis-based self-oscillation [3, 4], but any theoretical analysis for the phase-shifting self-oscillation has not yet been reported. This paper intends to reveal a very simple mathematical model of the oscillation frequency variation for a combined structure of the time delay, the hysteresis control, and the phase-shifting in feedback filter.

## II. SWITCHING FREQUENCY ANALYSIS

### A. Switching Frequency Variation

When the loop gain in the oscillation range is large enough, the oscillation is always settled by the phase condition (Barkhausen's criteria);

$$180^\circ = \angle \text{integrator}(\theta_{int}) + \angle \text{feedback filter}(\theta_o) + \angle \text{hysteresis delay}(\theta_h) + \angle \text{time delay}(\theta_{td}) \quad (1)$$

It is possible that the phase shift at the 1st-order integrator  $\theta_{int} = \pi/2$  [rad/s] at the oscillating frequency ( $f = f_{osc}$ ). With the adoption of a 1st-order passive filter, the phase shift (in degree) at the feedback filter is

$$\theta_o = \frac{180}{\pi} \cdot \tan^{-1}\left(\frac{f_{osc}}{f_o}\right) \quad (2)$$

as well as the proportionality between time delay and phase shift derives.

$$\theta_h = 360 \cdot \frac{h f_{osc}}{\omega_u}, \quad \theta_{td} = 360 \cdot \frac{f_{osc}}{f_D} \quad (3)$$

where  $f_D = 1/t_D$ .

A pulse-width modulated signal can be represented by the modulation depth (modulation index)  $M$  which is defined between +1 and -1, and related to its duty cycle  $D$  as  $M = 2 \cdot D - 1$ . The time delay and the hysteresis delay in Fig. 1(a) are known to be dependent on the input amplitude (consequently, modulation depth  $M$ ) [3, 4] given by:

$$\text{time delay} = \frac{t_D}{1 - M^2}, \quad \text{hysteresis delay} = \frac{h \cdot \tau_{int}}{1 - M^2} \quad (4)$$

where  $t_D$ , and  $h \tau_{int}$  are measured when  $M = 0$ .

These simple equations are verified perfect match with the system-level simulations in the audio band [3, 4]. The delay (phase shift) caused by the feedback filter, on the other hand, is less dependent on  $M$  as the input to the feedback filter is a digital pulse.

Therefore, the oscillation criterion derived from (1) to (4) is given by [rad/s]:

$$\pi = \frac{\pi}{2} + \tan^{-1}\left(\frac{f_{osc}}{f_o}\right) + \frac{2\pi f_{osc}}{1 - M^2} \left(\frac{h}{\omega_u} + \frac{1}{f_D}\right) \quad (5)$$

Seemingly, the feedback filter term (arc-tangent term) is not dependent on  $M$  in (5).

### B. Oscillating Frequency Model

Arc-tangent approximation: To obtain the simplified expression for  $f_{ox}$ , the arc-tangent function in (5) is approximated. Three different polynomial functions can be utilized to approximate the arc-tangent function over the range of the argument (angle) [5].

Over the different ranges of  $0^\circ \sim 45^\circ$ ,  $0^\circ \sim 60^\circ$ , and  $80^\circ \sim 90^\circ$ , the approximation is, respectively, given by:

$$\tan^{-1}\left(\frac{f_{osc}}{f_o}\right) \approx \frac{\pi}{4} \left(\frac{f_{osc}}{f_o}\right) \quad (6)$$

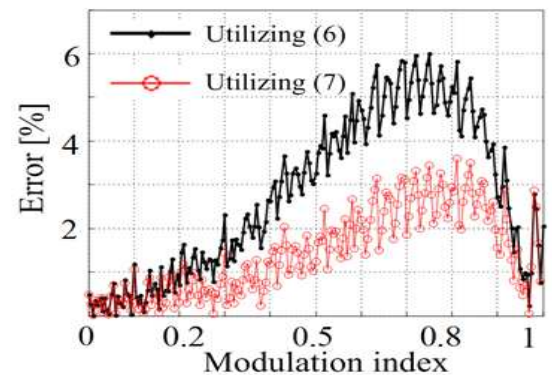
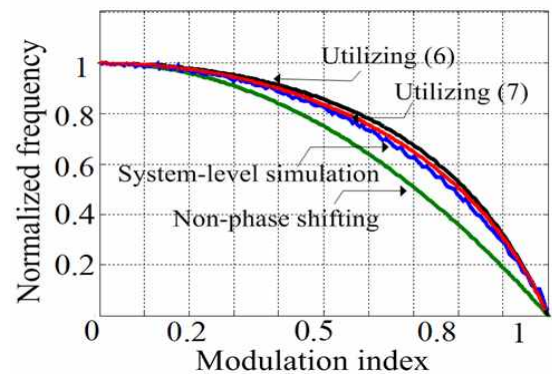
$$\tan^{-1}\left(\frac{f_{osc}}{f_o}\right) \approx \frac{\pi}{4} \left(\frac{f_{osc}}{f_o}\right) + 0.273 \left(\frac{f_{osc}}{f_o}\right) \left(1 - \frac{f_{osc}}{f_o}\right) \quad (7)$$

$$\tan^{-1}\left(\frac{f_{osc}}{f_o}\right) \approx \frac{\pi}{2} - \frac{\frac{f_{osc}}{f_o}}{1 + 0.28086 \left(\frac{f_{osc}}{f_o}\right)^2} \quad (8)$$

The oscillation frequency is now approximated in each segmentation, e.g. in the range of  $0^\circ \sim 45^\circ$  the simplified expression is derived from (5) and (6):

$$f_{osc} \approx \frac{2\omega_u f_o f_D (1 - M^2)}{\omega_u f_D (1 - M^2) + 8f_o (\omega_u + h \cdot f_D)} \quad (9)$$

The calculated oscillating frequencies with errors deviated from the system-level simulations in Matlab based on Fig. 1(a) are shown in Fig. 2(a), Fig. 2(b), and Fig. 2(c) for phase shifting =  $45^\circ$ ,  $60^\circ$  and  $85^\circ$ , respectively. More accurate results are obtained utilizing (7) rather than (6) for  $45^\circ$ , and  $60^\circ$ . Non-phase shifting curve in Fig. 2(a) is measured when the feedback filter term is excluded in (5). As expected, the oscillation frequency in this case drops more rapidly as  $M$  increases.



(a)

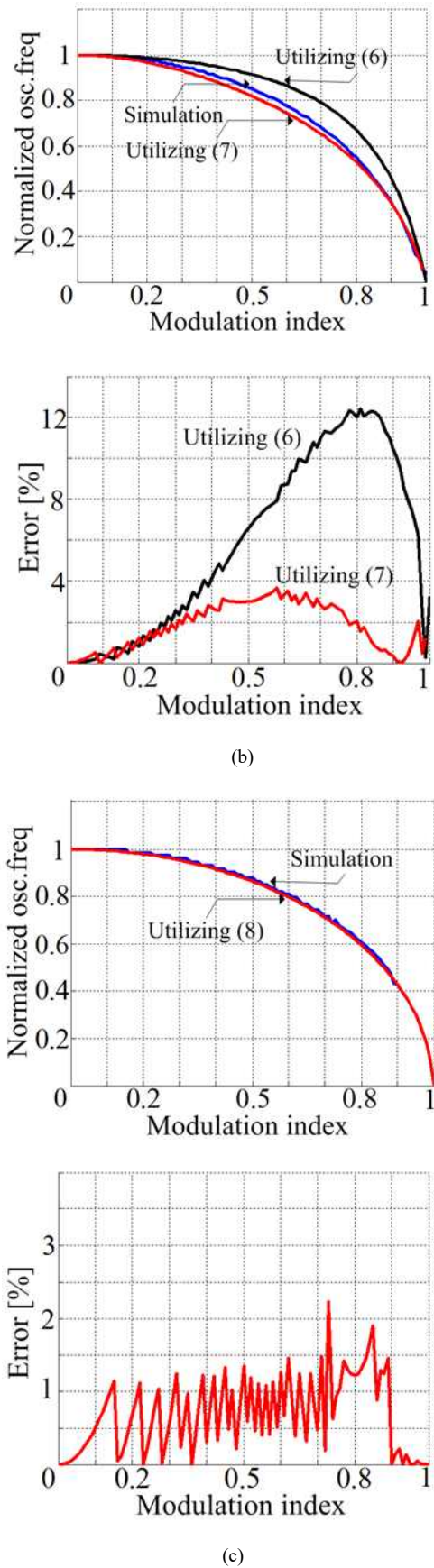


Fig. 2. Fluctuation of oscillation frequency and percentage error depending on modulation index (a) phase shift = 45° (b) phase shift = 60° (c) phase shift = 85°.

The non-phase shifting curve in Fig. 2(a) is measured when the feedback filter term is excluded in (5). As expected, the oscillation frequency in this case drops more rapidly as  $M$  increases.

### III. CIRCUIT DESIGN AND SIMULATION RESULTS

#### A. Adoption of Double Poles in Phase-Shifting Filter

Fig. 3(a) presents the proposed amplifier with multiple-pole feedback filter. From the perspective of phase shift, it contains a second-order integrator without the subsequent attenuator, a comparator, and the double-pole feedback filter. Fig. 3(b) and (c) show the employed integrator and comparator. The dual supply voltages ( $K > 1$ ) to provide the output stage with the higher supply voltage is used to transfer more power to the load.

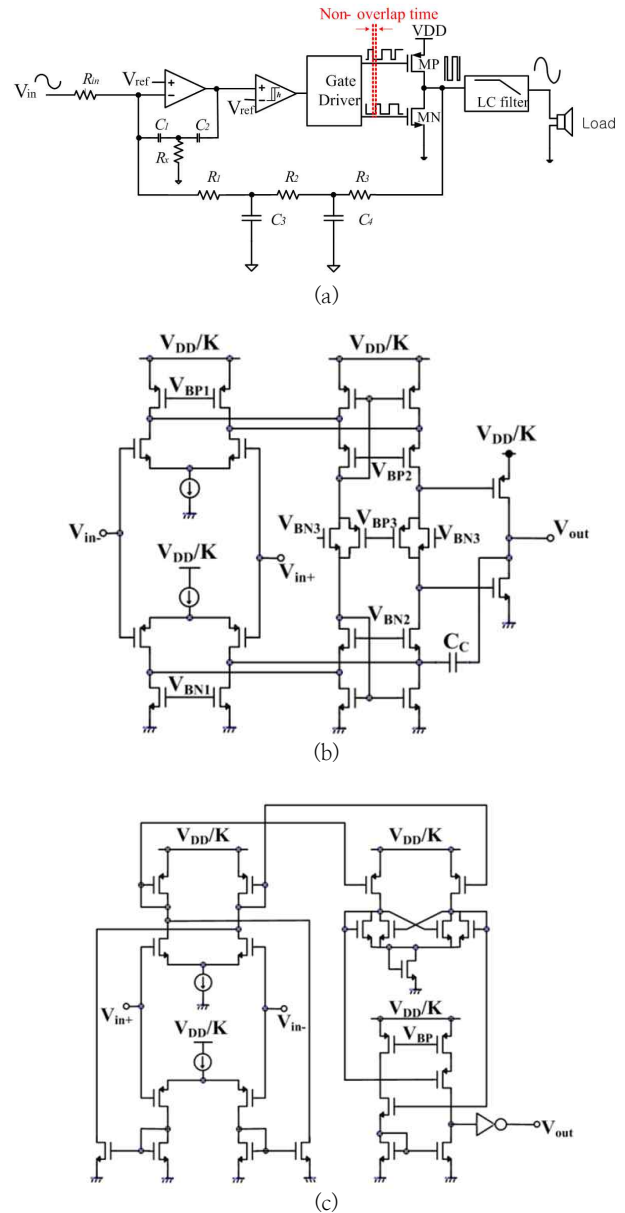


Fig. 3. Proposed architecture (a) circuit diagram adopting double pole phase-shifting loop filter (b) integrator (c) comparator.

The proposed modulator was implemented in a  $0.35\mu\text{m}$ -CMOS process with  $V_{\text{DD}} = 5\text{V}$ . As the switching transistors have very small on-resistance over  $0.4\sim 0.5\Omega$ , the dead time (non-overlap time) of about  $1.35[\text{ns}]$  was enforced to avoid the through current during the switching. The oscillation frequency is selected with  $C_1 = C_2 = 400[\text{fF}]$ ,  $C_3 = C_4 = 600[\text{fF}]$ ,  $R_{in} = 100[\text{k}\Omega]$ ,  $R_x = 1.5[\text{M}\Omega]$ ,  $R_1 = 100[\Omega]$ ,  $R_2 = R_3 = 300[\text{k}\Omega]$ .

Concerning the setback of the signal-dependent oscillation frequency, an attenuator with resistor string can be employed to reduce the dynamic range of the comparator input by limiting the variation range of  $t_d$ .

**B. Simulation Results**

The digital amp output falters as does the supply noise, and the oscillation frequency is near  $500\text{kHz}$ , as shown in Fig. 4(a) waveform (a) and (b). The signal reconstructed after the 4th-order Butterworth filter gets a dc gain of 2.8 as shown in Fig. 4(a) waveform (c). The spread-spectrum characteristic of the oscillation frequency is seen as intended for the better EMI. (See Fig. 4(b).) Another feature to note is the suppression of the supply noise through the feedback path. The larger supply noise than the signal gets reduced by more than  $30[\text{dB}]$ .

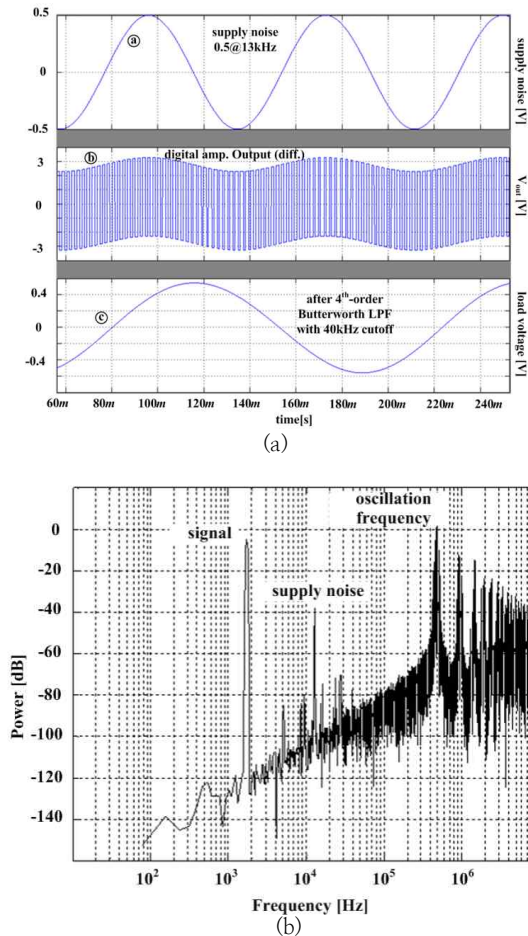


Fig. 4. Simulation results when a sinusoidal input of  $0.2\text{V}$  at  $1.3\text{kHz}$  is enforced (a) time-domain waveform (b) PSD of digital amp output waveform.

Table I shows the performance summary of the proposed scheme in conjunction with a prior work [4]. The proposed scheme adopting the 2nd-order integrator shows a better performance than the 1st-order integrator.

Table I.  
Performance comparison with prior works.

	[4]	This work
technology	$0.25\mu\text{m}$	$0.35\mu\text{m}$
supply voltage	$2.3 \sim 5.5 [\text{V}]$	$3.3 \sim 5 [\text{V}]$
$f_{\text{sw}}(M=0.8)/f_{\text{sw}}(M=0)$	0.6	0.8
PSRR	65 [dB]	74 [dB]
SNR	91.7 [dB]	123 [dB]
THD + N	-	0.0019 [%]
efficiency	88 [%]	90 [%]
power consumption	$3.88\text{mA}@3.6\text{V}$	$2.5\text{mA}@3.3\text{V}$
Active die area	$1.6 \text{mm}^2$	$0.77 \text{mm}^2$

**IV. CONCLUSIONS**

A mathematical model used for self-oscillating class-D audio amplifiers including phase-shifting, time delay, and hysteresis window is proposed. It depicts the oscillating frequency variation in terms of the modulation depth, which shows that more portion of phase shift in the feedback filter than the other two terms is desirable from the perspective of the less variation. The phase shifting of the loop filter is assorted into three different angular regions. The proposed model for  $45^\circ$ ,  $60^\circ$  and  $85^\circ$  was presented with the behavioral-level simulations. The margin of less than 5% error was reported with the proper choice of model.

The main feature of the self-oscillation scheme lies in a relatively lower switching (oscillating) frequency of several hundreds of kilo Hertz, tracking the input amplitude more or less. Thus, it generates less quantization noise and idle tones than a PWM or a delta-sigma modulator of the same order.

The proposed self-oscillating scheme has basically a delta-sigma nature, leading to a higher oscillation frequency than the PWM method. While the higher-order loop gain contributes to the high PSRR and THD, the aspect of the stable oscillation frequency according to the input amplitude variation is particularly revealed. The validity of the proposed scheme is proved based on Spectre simulations using  $0.35\text{-}\mu\text{m}$  CMOS process. It achieved a PSRR of  $-74\text{dB}$  at  $1\text{kHz}$  and a THD+N well below  $0.0019\%$  between  $10\text{Hz}$  and  $20\text{kHz}$ . The active chip area is  $0.77\text{m}^2$  and the power consumption is  $8.25\text{mW}$ .

## REFERENCES

- [1] P. Hulst, A. Veltman, and R. Groenenberg, *112<sup>th</sup> Conv. Audio Engineering Society*, (Munich, Germany, May, 2002) pp. 1–7.
- [2] A. Matamura, N. Nishimura, and B.Y. Liu, *Proc. ISCAS*, (2009) pp. 1177–1180.
- [3] M. Berkhout, and L. Dooper, *IEEE Trans. Circuits and Syst.*, **57** pp. 992–1002 (2010).
- [4] A. Huffenus, G. Pillonnet, N. Abouchi, F. Goutti, V. Rabary, and C. Specq, *Proc. ISCAS*, (2010) pp. 769–772.
- [5] S. Rajan, S. Wang, R. Inkol, and A. Joyal, *IEEE Signal Processing Magazine*, **23** pp. 108–111 (2006).
- [6] B. Putzeys, *118<sup>th</sup> Conv. Audio Engineering Society*, May 2005, Preprint 6453
- [7] van der Hulst, Paul; Veltman, Andre; Groenenberg, Rene, *112<sup>th</sup> AES Convention*, Preprint 5503
- [8] Frederiksen, Thomas; Bengtsson, Henrik; Nielsen, Karsten, *109<sup>th</sup> AES Convention*, Preprint 5197
- [9] F. Nyboe, *27<sup>th</sup> AES Convention*, September 2005



**Hyunsun Mo** received the B.S., M.S., and Ph.D degrees in Electronic Engineering from Kookmin University, Seoul, Korea, in 1993 and 2011, and 2014, respectively. In 1993, she joined Samsung Electronics Semiconductor Division of the development of the low power and high-speed SRAM and Flash memory circuits. Her

research interests include the design of analog circuits, power-management ICs, and the next-generation memories.



**Daejeong Kim** received the M.S. and Ph.D. degree in electronic engineering from Seoul National University, Seoul, Korea, in 1989 and 1994, respectively. In 1994, he joined LG Semicon Co. Ltd., Korea, as an integrated circuit design engineer. Since 1999, he has been with the School of Electrical Engineering, Kookmin

University, Seoul, Korea. His research interests are analog integrated circuits and integrated power electronics.